

Figure Sources

- p. 2 Chart derived from Google Ngram Viewer: LIDAR versus lidar versus LiDAR versus LADAR (1950–2008, English).
- p. 10 top http://en.wikipedia.org/wiki/Laser_safety. Public domain.
- p. 10 bottom http://en.wikipedia.org/wiki/Laser_safety. Figure created by Han-Kwang Nienhuys and released under license CC-BY-2.5.
- p. 11 http://en.wikipedia.org/wiki/Laser_safety. Figure created by Dahn and released under licence CC-BY-2.5.
- p. 18 Figure created by R. Pogge from ATRAN model data of Lord, S.D. (1992, NASA Technical Memor. 103957) from the Gemini Observatory website (<http://www.gemini.edu>).
- p. 19 top © Mike Willis December 26th, 2006.
- p. 19 bottom © The Worlds of David Darling.
- p. 27 Courtesy of Agilent Technologies.
- p. 30 http://en.wikipedia.org/wiki/Pink_noise. Figure created by Marrakkk and released under license CC BY-SA 3.0.
- p. 40 Courtesy of Matthew Dierking, Air Force Research Lab.
- p. 47 P. McManamon, “Review of ladar: A historic, yet emerging, sensor technology with rich phenomenology,” *Opt. Eng.* **51**(6), 060901 (2012) [doi: 10.1117/1.OE.51.6.060901].
- p. 52 National Research Council, *Laser Radar: Progress and Opportunities in Active Electro-Optical Sensing*, The National Academies Press, Washington, D.C., p. 63 (2014).
- p. 53 National Research Council *Laser Radar: Progress and Opportunities in Active Electro-optical Sensing*, The National Academies Press, Washington, D.C., p. 88 (2014).
- p. 54 R. C. Hardie, M. Vaidyanathan, and P. F. McManamon, “Spectral band selection and classifier design for a multispectral imaging laser radar,” *Opt. Eng.* **37**(3), 752–762 (1998) [doi: 10.1117/1.601907].

Figure Sources

- p. 58 Adapted from J. C. Marron and R. L. Kendrick, "Distributed aperture active imaging," *Proc. SPIE* **6550**, 65500A (2007) [doi: 10.1117/12.724769].

p. 68 Courtesy of Jeff Hecht.

p. 73 top <http://en.wikipedia.org/wiki/Mode-locking>. Released under license CC BY-SA 3.0-MIGRATED.

p. 79: R. V. Chimenti, M. P. Dierking, P. E. Powers, and J. W. Hausa, "Multiple chirp sparse frequency LFM ladar signals," *Proc. SPIE* **7323**, 73230N (2009) [doi: 10.1117/12.817865].

p. 87 Courtesy of Intevac, Inc. <http://www.intevac.com/intevacphotonics/ebaps-technology-overview/>. Figure reprinted with permission.

p. 93 Courtesy of How Stuff Works: <http://science.howstuffworks.com/gimbal1.htm>.

p. 96 Courtesy of Nikon Small World: <http://www.microscopyu.com/articles/confocal/resonantscanning.html>.

p. 97 P. F. McManamon, P. J. Bos, M. J. Escuti, J. Heikenfeld, et al., "A review of phased array steering for narrow-band electro-optical systems," *Proc. IEEE* **97**(6), 1078–1096 (2009).

p. 100 P. F. McManamon, P. J. Bos, M. J. Escuti, J. Heikenfeld, et al., "A review of phased array steering for narrow-band electro-optical systems," *Proc. IEEE* **97**(6), 1078–1096 (2009).

p. 104 P. F. McManamon, P. J. Bos, M. J. Escuti, J. Heikenfeld, et al., "A review of phased array steering for narrow-band electro-optical systems," *Proc. IEEE* **97**(6), 1078–1096 (2009).

p. 105 top S. R. Davis, G. Farca, S. D. Rommel, S. Johnson, and M. H. Anderson, "Liquid crystal waveguides: New devices enabled by >1000 waves of optical phase control," *Proc. SPIE* **7618**, 76180E (2010) [doi: 10.1117/12.851788].

p. 105 bottom S. R. Davis, G. Farca, S. D. Rommel, S. Johnson, and M. H. Anderson, "Liquid crystal waveguides: New devices enabled by >1000 waves of optical phase control," *Proc. SPIE* **7618**, 76180E (2010) [doi: 10.1117/12.851788].

Figure Sources

- p. 107 P. F. McManamon, P. J. Bos, M. J. Escuti, J. Heikenfeld, et al., “A review of phased array steering for narrow-band electro-optical systems,” *Proc. IEEE* **97**(6), 1078–1096 (2009).
- p. 108 top P. F. McManamon, P. J. Bos, M. J. Escuti, J. Heikenfeld, et al., “A review of phased array steering for narrow-band electro-optical systems,” *Proc. IEEE* **97**(6), 1078–1096 (2009).
- p. 108 bottom P. F. McManamon, P. J. Bos, M. J. Escuti, J. Heikenfeld, et al., “A review of phased array steering for narrow-band electro-optical systems,” *Proc. IEEE* **97**(6), 1078–1096 (2009).
- p. 109 P. F. McManamon, P. J. Bos, M. J. Escuti, J. Heikenfeld, et al., “A review of phased array steering for narrow-band electro-optical systems,” *Proc. IEEE* **97**(6), 1078–1096 (2009).
- p. 110 E. A. Watson, “Analysis of beam steering with decentered microlens arrays,” *Opt. Eng.* **32**(11), 2665–2670 [doi: 10.1117/12.148100].
- p. 113 Courtesy of Raytheon.
- p. 115 http://en.wikipedia.org/wiki/Inertial_measurement_unit. Released under license CC BY-SA 3.0.
- p. 118 <http://en.wikipedia.org/wiki/Aliasing>. Released under license CC BY-SA 3.0.
- p. 122 P. McManamon, “Review of lidar: A historic, yet emerging, sensor technology with rich phenomenology,” *Opt. Eng.* **51**(6), 060901 (2012) [doi: 10.1117/1.OE.51.6.060901].

Bibliography

- Alexander, S. B., *Optical Communication Receiver Design*, SPIE Press, Bellingham, Washington (1997) [doi: 10.1117/3.219402].
- Beck, S., J. Buck, W. Buell, R. Dickinson, D. Kozlowski, N. Marechal, and T. Wright, "Synthetic aperture imaging laser radar: Laboratory demonstration and signal processing," *Appl. Opt.* **44**(35), 7621–7629 (2005).
- Fox, C. S., Ed., *Active Electro-Optical Systems*, in *The Infrared & Electro-Optical Systems Handbook*, Vol. 6, J. S. Accetta and D. L. Shoemaker, Eds., Environmental Research Institute of Michigan, Ann Arbor, Michigan and SPIE Optical Engineering Press, Bellingham, Washington (1993).
- S. B. Compana, Ed., *Passive Electro-Optical Systems, The Infrared and Electro-Optical Systems Handbook*, Vol. 5, J. S. Accetta and D. L. Shoemaker, Eds., Environmental Research Institute of Michigan, Ann Arbor, Michigan and SPIE Optical Engineering Press, Bellingham, Washington (1993).
- Fujii, T. and T. Fukuchi, Eds., *Laser Remote Sensing*, Taylor and Francis Group, Boca Raton, Florida (2005).
- Henderson, S. W., P. Gatt, D. Rees, and M. Huffaker, "Wind LIDAR," Chapter 7 in *Laser Remote Sensing*, T. Fujii and T. Fukuchi, Eds., Taylor and Francis Group, Boca Raton, Florida (2005).
- Jelalian, A. V., *Laser Radar Systems*, Artech House, Norwood, Massachusetts (1991).
- Keyes, R. J., "Heterodyne and nonheterodyne laser transceivers," *Rev. Sci. Instrum.* **57**, 519 (1986).
- Krause, B., J. Buck, C. Ryan, D. Hwang, P. Kondratko, A. Malm, A. Gleason, and S. Ashby, "Synthetic aperture lidar flight demonstration," CLEO 2011, Laser Applications to Photonic Applications, PDPB7, Optical Society of America, Washington, D.C. (2011).

Bibliography

- Marron, J. C., R. L. Kendrick, N. Seldomridge, T. D. Grow, and T. A. Hoft, "Atmospheric turbulence correction using digital holographic detection: Experimental results," *Opt. Exp.* **17**, 11638 (2009).
- McManamon, P. F. "Review of lidar: A historic, yet emerging, sensor technology with rich phenomenology," *Opt. Eng.* **51**(6), 060901 (2012) [doi: 10.1117/1.OE.51.8.089801].
- McManamon, P. F., G. Kamerman, and M. Huffaker, "A history of laser radar in the United States," *Proc. SPIE* **7684**, 76840T (2010) [doi: 10.1117/12.862562].
- National Research Council, *Laser Radar: Progress and Opportunities in Active Electro-Optical Sensing*, The National Academies Press, Washington, D.C. (2014).
- Osche, G. R., *Optical Detection Theory for Laser Applications*, Wiley-Interscience, New York (2002).
- Overbeck, J. A., M. S. Salisbury, M. B. Mark, and E. A. Watson, "Required energy for a laser radar system incorporating a fiber amplifier or an avalanche photodiode," *Appl. Opt.* **34**, 7724–7730 (1995).
- Reibel, R. R., P. A. Roos, T. J. Berg, B. Kaylor, N. Greenfiend, Z. W. Barber, C. J. Renner, and W. R. Babbit, "Ultra-broadband optical chirp linearization for precision length metrology applications," Optical Fiber Communication Conference, 2010, Optical Society of America, Washington, D.C., OThQ2 (2010).
- Richmond, R. D. and S. C. Cain, *Direct-Detection LIDAR Systems*, SPIE Press, Bellingham, Washington (2010) [doi: 10.1117/3.836466].
- Siegman, A. E., "The antenna properties of optical heterodyne receivers," *Proc. IEEE* **54**(10), 1350–1356 (1966).

Index

- 1D lidar, 3
 1D slices, 41
 1D waveguide, 66
 1D waveguide lasers, 66
 $1/f$ noise, 7, 30
 2D lidar, 2, 42
 3D lidar, 3
 3D mapping, 4, 43
 3D point cloud images, 127
 3D scanning lidars, 43
 3D shape, 127
 3D shape information, 43
 3D voxels, 122, 127
- absolute motion, 115
 absorption, 109
 accelerometers, 115
 acousto-optic devices, 85
 acousto-optic modulator, 85
 active cladding layer, 105
 active multispectral imaging, 54
 adaptive optics mirror, 22
 aero-optical effect, 21
 aero-optical layer, 21
 afterpulsing, 32
 Airy disk, 92
 all-positive lenslet approach, 112
 amplification stages, 75
 amplitude variations, 22
 angle information, 41
 angular distribution, 41
 angular resolution, 59
 angular rotation, 50
 applied voltage, 99
 archeological mapping, 4
 artificial gain medium, 68
- atmospheric absorption, 18
 atmospheric coherence time, 20
 atmospheric loss, 19
 atomic constituents, 52
 autocorrelation, 124
 avalanche gain, 31
 avalanche photodiode, 30–31, 44–45, 82
- background noise, 29
 band structure engineering, 68
 bandwidth of the lidar, 40
 beam, 8
 beam quality, 74
 birefringence, 99
 bistatic lidar, 1, 12, 61
 blue shift, 90
 bulk defects, 30
 bulk solid state lasers, 64
- carrier-to-noise ratio, 37
 cascade diode lasers, 67
 cellular network planning, 4
 central limit theorem, 26
 chip, 80, 102
 chirping, 47
 circularly polarized gratings, 107
 cladding, 65
 Class 1 lasers, 11
 Class 2 lasers, 11
 Class 3 lasers, 11
 Class 3B lasers, 11
 Class 4 lasers, 11
 clock frequency drifts, 117

Index

- CO₂, 6, 18
 CO₂ laser, 61
 code division multiple access, 80
 coherence converters, 61
 coherence length, 9
 coherent detection, 84
 coherent detection system, 41
 coherent lidar, 1, 3, 7, 24, 28
 coherent receiver, 34
 coincidence processing, 45
 coincident returns, 32
 conformal steering approach, 95
 constant fraction detection, 119
 controlled laser modes, 66
 convolution, 117
 corner cubes, 15
 cross section, 14
 cross section of a corner cube, 16
 dark current, 30
 dark current noise, 30
 dark frame subtraction, 30
 dead time, 83
 deflection efficiency, 85
 deformable mirror, 22
 degree of polarization, 55
 delta function, 89
 detector angular subtense, 3, 92, 114
 differential absorption lidar, 5
 diffraction limit, 8
 digital beam steering, 109
 digital convolution, 117
 digital holography, 7, 33
 dihedral, 16
 diode, 65
 diode lasers, 61, 67
 direct detection, 7, 23, 25, 31
 direct detection lidar, 24, 81
 direct detection receiver, 34
 direction of the illumination, 55
 discrete Poisson probability density function, 26
 Doppler lidar, 5
 Doppler shift, 48, 77, 90, 126
 Doppler shift measurement time, 90
 Doppler spectrum, 41
 doublet pulse waveform, 78
 dual-frequency liquid crystals, 99
 edge-emitting diode lasers, 67
 effective aperture, 59
 effective grayscale, 83
 effective range profile, 83
 effectively apodized aperture array, 59
 electrical singal-to-noise ratio, 25
 electro-optical scanning, 106

Index

- electron-bombarded
 active-pixel sensor, 87
 electron-bombarded
 semiconductor, 87
 electronic levels, 53
 electrowetting, 104
 emission spectrum, 52
 emission wavelengths, 52
 end pumping, 69
 energy received equation,
 23
 Er:YAG lasers, 64
 excess noise, 30
 excess noise factor, 30
 eye damage threshold, 10
 eye safety, 10
 eyesafe region, 64
- fast Fourier transform,
 121
 fast-steering mirror, 94
 ferroelectric liquid
 crystals, 109
 fiber laser, 65
 fiber lasers, 61
 fiber tip damage, 66
 field of view, 3
 fill factor, 103
 fixed-pattern noise, 30
 flash image, 115
 flash imagers, 44
 flash imaging, 1
 flash imaging with lidar,
 88
 flash lidar, 12
 flashlamps, 69
 flicker noise, 30
 flyback region, 100
 FM chirp, 77
- focal spot, 116
 focal spot diameter, 114
 focusing ability, 114
 forestry lidar, 4
 forward-looking infrared
 cameras, 86
 four-level laser, 63
 Fourier transform, 121
 frequency chirping, 89
 frequency division
 multiple access, 80
 frequency line shape, 73
 frequency shifting, 76
 Fresnel loss, 109
 Fried parameter, 20
 fringing fields, 100–101
 frozen atmosphere
 assumption, 20–21
- gain medium, 75
 gain region, 65
 gamma distribution, 26
 gated 2D camera, 42
 gated 2D imaging, 87
 gating circuitry, 42
 Gaussian beam, 8
 Gaussian illumination, 98
 Gaussian probability
 density function, 26
 Gaussian-shaped pulse,
 118
 Geiger-mode APD, 23, 83,
 115
 Geiger-mode APD camera,
 122
 Geiger-mode lidar, 125
 general image quality
 equation, 123
 geometrical optics, 114

Index

- gimbal pointing, 93
 gimbals, 21, 93
 GMAPD detection events, 32
 GMAPD flash imagers, 45
 GMAPD-based flash imaging, 45
 gyroscopes, 115
- half-power point, 98
 hard targets, 54
 heterodyne detection, 23, 89
 heterodyne detection receiver, 34
 heterodyne mixing efficiency, 35
 HgCdTe, 46
 high range resolution, 47
 high time-bandwidth product waveform, 78
 high time-bandwidth product waveforms, 77
 high-duty-cycle waveforms, 67
 high-gain laser media, 75
 high-index oil, 104
 hill climbing algorithm, 58
 HoTm:YAG lasers, 64
- illuminator aperture, 12
 imposing the small motion, 116
 in-plane steering, 105
 index of refraction, 20
 index of refraction change, 72
- inertial measurement unit, 115
 interband lasers, 67
 interference, 17, 56
 intermediate frequency, 36–37
 inverse synthetic aperture lidar, 50
 inverse synthetic aperture radar, 50
 irradiation, 52
 isolation, 75
 isoplanatic angle, 20
 isoplanatic patch, 20
- Johnson noise, 27
 Johnson's criteria, 123
- Kerr-effect EO crystals, 106
 KTN, 106
- LADAR, 2
 Lambertian scattering, 29
 large-angle steering, 113
 largest angle that can be steered, 98
 laser beam divergence, 8
 laser designators, 6
 laser diodes, 6
 laser imaging and ranging, 72
 laser linewidth, 74
 laser pulse, 77
 laser radar, 2
 laser radiation, 10
 laser range finders, 6
 laser remote sensing, 2
 laser resonator, 62

Index

- laser signal, 1
 laser vibrometer, 48
 laser vibrometer signal processing, 126
 laser vibrometry, 126
 laser waveform, 1
 laser-induced breakdown spectroscopy, 5, 52
 laser-induced fluorescence, 5
 laser-induced fluorescence lidar, 53
 leading edge detection, 119
 lensless imaging, 121
 lenslet-based beam steering, 110
 Level 0 (L0), 125
 Level 1 (L1), 125
 Level 2 (L2), 125
 Level 3 (L3), 125
 Level 4 (L4), 125
 Level 5 (L5), 125
 lidar, 1–2
 lidar clock frequency, 117
 lidar cross section, 15
 lidar data processing stages, 125
 lidar development, 6
 lidar image stabilization, 88
 lidar peak power, 66
 lidar pulse, 89
 lidar range equations, 14
 lidar range resolution, 89
 lidar waveform, 77
 lidar wavelengths, 18
 LIMAR, 86
 LiNbO_3 , 106
 line broadening, 73
 linear EO crystals, 106
 linear EO effect, 106
 linear FM waveforms, 80
 linear frequency modulation, 79, 89
 linear-mode APD, 23, 46, 82, 122
 liquid crystal layer, 100
 liquid crystal polarization gratings, 108
 liquid crystal steering device, 99
 local oscillator, 28, 33, 37
 local oscillator power, 24
 long-focal-length optics, 114
 long-integration-time framing cameras, 86
 low energy per pulse, 83
 low-index water, 104
 master oscillator, 75
 master oscillator, power amplifier, 75
 matched filter, 117
 maximum permissible exposure, 10–11
 measured range profile, 117
 MEMS mirror, 94
 MEMS mirror arrays, 103
 MEMS-mirror-based steering, 103
 micro-actuators, 103
 microlens array, 110
 micromotion, 116
 Mie scattering, 19
 mixed set of lenslet arrays, 112

Index

- mixed-lenslet steering,
 112
 mixed-pixel effect, 55
 mode-locked lasers, 73
 modulo 2π beam steering,
 97
 modulo 2π phase profile,
 97
 monochromaticity, 9
 monostatic lidars, 1, 12
 Mueller matrix
 characterization, 55
 multiple input, multiple
 output lidars, 12
 multiple pulses, 83
 multiple subapertures, 124
 multiple tagged laser
 transmitters, 76
 multiple-aperture lidars,
 57
 multiple-input, multiple-
 output lidars, 57, 59
- nanofabricated phased
 arrays, 102
 National Imagery
 Interpretability
 Rating Scale, 123
 Nd:YAG designators, 64
 Nd:YAG lasers, 61, 64
 negative binomial
 distribution, 26
 nitrogen, 18
 noise current, 24
 noise equivalent photons,
 87
 noise equivalent
 temperature
 difference, 87
- noise probability density
 functions, 26
 nonlinear effects, 70
 number of photons, 32
 numerical aperture, 114
 Nyquist criterion, 118
 Nyquist noise, 27
 Nyquist sampling
 theorem, 118
- object identification, 127
 oil and gas exploration, 4
 optical breakdown, 52
 optical parametric
 amplifier, 70
 optical parametric
 oscillator, 70
 optical path difference, 97
 optical phased arrays, 57
 optical power received, 14
 optimal wavelengths, 54
 order of the blaze, 104
 out-of-plane steering, 105
 overall laser efficiency, 75
 oxygen, 18
- pattern of changes, 91
 peak detection, 119
 peak-power limitation, 65
 periodically poled lithium
 niobate, 70
 phase center, 49
 phase change, 22
 phase correction, 22
 phase corrector plates, 110
 phase delay, 111
 phase function, 92
 phase irregularities, 56
 phase profile, 92

Index

- phase screen, 92
 phase shift interferometry,
 7
 phase steps, 101
 phase up the multiple
 subapertures, 60
 phased array of phased-
 array imaging, 57
 photon, 28
 photonic crystal fiber
 lasers, 66
 photonic crystal fibers,
 65–66
 pink noise, 30
 pitch, 115
 Pockels cell, 47, 71–72
 point spread function, 3, 92
 polarimetric
 measurements, 55
 polarization, 13, 55
 polarization-based flash
 lidar imaging, 47
 polarization-encoded
 imaging, 44
 polarizing beamsplitter,
 13
 polygon scanning, 96
 polymers, 99
 polypulse waveform, 78
 population inversion, 63
 power received equation,
 23
 precise object
 identification, 4
 preform, 65
 pseudo-random-coded
 modulation, 77, 89
 pseudo-random-coded
 waveform, 80
 pulse doublet, 77–78
 pulse position modulation,
 80
 pulsed ultraviolet sources,
 53
 Q, 71
 Q switching, 71
 Q-switched lasers, 42
 quadratic Kerr effect, 106
 quadrature detection, 36
 quantization loss, 101
 quantum cascade lasers,
 68
 quantum defect, 63
 quarter-wave plate, half-
 wave plate, quarter-
 wave plate, 107
 quasi-cw operation, 64
 quasi-four-level lasers, 63
 radiance, 14
 radiance per wavelength,
 29
 Raman lidar, 5
 random interference, 9
 range, 3
 range accuracy, 120
 range depth, 79
 range Doppler imaging, 51
 range information, 41, 47
 range measurement
 accuracy, 117
 range precision, 120
 range profile, 40
 range resolution, 3, 40, 120
 range uncertainty, 79
 range-gated active
 imaging, 42

Index

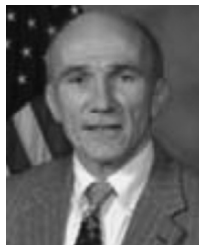
- range-only lidar, 3
 range-resolved data, 53
 range/species resolution,
 53
 Rayleigh scattering, 19
 read-out integrated
 circuit, 82
 receive aperture, 12
 receive-only arrays, 57
 receiver, 13
 reconstruct the range
 profile, 118
 red shift, 90
 reference beam, 36
 reference frame
 adjustment, 50
 reflective or transmissive
 modes, 104
 relative motion, 115
 relative time delay, 40
 required transmitted
 energy, 23
 retina, 10
 RF modulation, 81
 Risley gratings, 95
 Risley prisms, 95
 roll, 115
 rotating phase, 108
 rotating polygons, 96
 rotation speed, 41
 route planning, 4

 sag formula, 111
 sampling density, 116
 saturable absorber, 71
 sawtooth phase profile, 97
 scanning lidars, 122
 scatter, 109
 seeding a laser, 74

 series of sine waves, 118
 shot noise, 27–28
 side pumping, 64, 69
 signal current, 24
 signal-to-noise equation,
 25, 39
 signal-to-noise ratio,
 23–24, 37, 82
 single detector, 51
 slip rings, 93
 solid angle return, 16
 solid state lasers, 61
 spatial coherence, 8
 spatial fringes, 35
 spatial heterodyne
 detection, 7, 33, 38–39,
 86, 124
 spatial heterodyne
 imaging, 58
 speckle, 9, 17
 speckle imaging lidar, 56
 speckle pattern, 56
 speckle realization, 17
 spectroscopic analysis, 52
 spontaneous emission, 63
 spurious sidelobes, 102
 stabilization, 43
 stable resonators, 62
 standard framing
 cameras, 47
 steering angle, 110
 steering efficiency, 101
 steering efficiency versus
 angle, 100
 steering loss, 109
 steering prisms, 95
 steering to discrete angles,
 110
 stimulated emission, 63

Index

- stitching, 115
 stochastic parallel
 gradient descent, 58
 Stokes vector, 55
 stretch processing, 79
 subapertures, 59
 sum and difference
 frequency generation,
 70
 super-Gaussian, 8
 super-Gaussian beam, 8
 surface of the eye, 10
 surface roughness, 55
 surveying, 4
 switching time, 99
 synthetic aperture
 imagers, 49
 synthetic aperture lidar, 3,
 49
 synthetic aperture radar,
 49
- target reflectivity, 14
 temporal coherence, 9
 temporal heterodyne
 detection, 7, 33–35,
 84–85
 temporal heterodyne
 imaging, 58
 temporal heterodyning, 48
 ternary steering, 108
 thermal noise, 27
 three-level laser, 63
 threshold detectors, 119
 Ti:sapphire laser, 73
 tilting, 103
 time analysis, 53
 time division multiple
 access, 80
- time gating, 52
 time tag, 89
 time-bandwidth product,
 78
 Tm:YAG lasers, 64
 tomographic images, 41
 transmissive beam
 steering, 104
 transmit and receive
 arrays, 57
 transmit aperture, 12
 transmit/receive isolation,
 13
 transmitter, 13
 transmitter array, 76
 trihedral, 16
 turbulence, 21
- unambiguous range, 47, 91
 uniform illumination, 98
 unstable resonators, 62
- velocity, 90
 vertical-cavity surface-
 emitting lasers, 67
 vibration, 48
 vibrational image, 48
 virtual phase screen, 22
 volume holographic
 gratings, 113
- water vapor, 18
 waveform generator, 1
 waveguide coupler, 105
 wide-angle steering, 110
- yaw, 115
- zero crossing, 95



Paul McManamon owns Exciting Technology LLC and is the Technical Director of Ladar and Optical Communications Institute (LOCI) at the University of Dayton. Dr. McManamon recently chaired the National Academy of Sciences (NAS) study “Laser Radar: Progress and Opportunities in Active Electro-Optical Sensing,” released in March, 2014. Dr.

McManamon co-chaired the NAS study, “Optics and Photonics: Essential Technologies for Our Nation,” released in August, 2012. This study recommended the National Photonics Initiative. He also served as Vice Chair to the 2010 NAS study “Seeing Photons.”

Dr. McManamon started at Wright-Patterson Air Force Base in May 1968 and retired from the same in 2008 as Chief Scientist of the Sensors Directorate, U.S. Air Force Research Laboratory (AFRL). Previous to that he was Senior Scientist of EO Sensors, and before that, acting chief scientist for Avionics, also at AFRL.

In 2006 he received the Meritorious Presidential Rank Award. He has participated in three Air Force Scientific Advisory Board studies. He was instrumental in the development of laser flash imaging to enhance EO target recognition range by a factor of 4 or 5. Dr. McManamon was the 2006 President of SPIE. He served on the SPIE Board of Directors for seven years and on the SPIE Executive Committee for four years. In 1998, Dr. McManamon and his co-authors received the IEEE W.R.G. Baker award for best paper in *any* refereed IEEE journal or publication. Dr. McManamon is a Fellow of SPIE, IEEE, OSA, AFRL, MSS, AIAA, and DEPS.